Magnetic hardening in as-cast Nd-rich Nd-Fe-B magnets

E. W. Singleton, A. Tsoukatos, Y. Zhang, and G. C. Hadjipanayis

Citation: Journal of Applied Physics **69**, 5820 (1991); doi: 10.1063/1.347860
View online: http://dx.doi.org/10.1063/1.347860
View Table of Contents: http://scitation.aip.org/content/aip/journal/jap/69/8?ver=pdfcov
Published by the AIP Publishing

Magnetic hardening in as-cast Nd-rich Nd-Fe-B magnets

E. W. Singleton, A. Tsoukatos, Y. Zhang, and G. C. Hadjipanayis
Department of Physics and Astronomy, University of Delaware, Newark, Delaware 19716

The microstructure of as-cast Nd-rich Nd-Fe-B alloys has been studied in detail and correlated with their magnetic hysteresis behavior. A hard magnetic phase with a Curie temperature around 250 °C and a coercivity of 5.2 kOe has been observed in an arc-melted $Nd_{80}Fe_{15}B_5$ sample. Annealing at around 600 °C led to a transformation of this phase to $Nd_2Fe_{14}B$ which is present in the form of small crystallites randomly disbributed in a nonmagnetic Nd-rich matrix, resulting in coercivities greater than 14 kOe. The Stoner and Wohlfarth model of single domain particles has been used to discuss the large coercivities.

I. INTRODUCTION

Recent studies on Nd-rich, Nd-Fe alloys with eutectic composition aimed at depicting the phase which is liquid at sintering temperatures have shown the existence of new anisotropic phases which originally were believed to be oxygen stablized.[1–7] A relatively high coercivity was found in as-cast Nd-Fe binary alloys and is attributed to a metastable phase[8,9] with a Curie temperature $T_c = 250$ °C which is magnetically hard. This phase has been observed as finely dispersed elongated and spherical particles ($\approx 5\ \mu$m) embedded in a nonmagnetic Nd-rich matrix. Another phase was also observed in as-cast binary Nd-Fe alloys with $T_c \simeq 230$ °C which is believed to be magnetically soft. Recently, Moreau *et al.*[10] determined the structure of the latter phase and found it to be hexagonal with composition Nd_5Fe_{17}. Studies show these phases to exist from very low Fe concentrations up to 20 at. % Fe.[5] In Nd-rich ternary Nd-Fe-B alloys, the magnetically hard metastable phase is also observed in as-cast samples and it is found to transform to $Nd_2Fe_{14}B$ after a heat treatment at around 500–600 °C.[8,9]

To obtain more information on the magnetic and structural properties of the ternary, Nd-rich, Nd-Fe-B alloys we have characterized a series of as-cast $Nd_{95-x}Fe_xB_5$ alloys with iron content ranging from 5 to 25 at. %. Particular emphasis was placed on samples with compositions near the Nd-Fe eutectic.

II. EXPERIMENT

The as-cast Nd-Fe-B alloys were obtained by arc-melting high-purity (at least 99.9%) Nd, Fe, and Fe-B under argon atmosphere. Small ingots of 3 g were used to ensure homogeneous compositions. The heat treatments were done in encapsulated quartz tubes under vacuum. Differential thermal analysis (DTA) provided information for the heat-treating temperatures.

Magnetic hysteresis measurements were made using a vibrating sample magnetometer (VSM) with fields of up to 14 kOe, and a SQUID magnetometer with fields up to 55 kOe and in the temperature range 10–300 K.

Scanning electron microscopy (SEM) and transmission electron microscopy (TEM) were used to examine the microstructure of several samples. Due to the ease of oxidation, special care was taken in sample preparation for microstructure studies.

III. RESULTS

Figure 1 shows the thermomagnetic $[M_H(T)]$ curves in the heating cycle [Fig. 1(a)] and cooling cycle [Fig. 1(b)] for alloys with compositions $Nd_{95-x}Fe_xB_5$. In the as-cast samples, thermomagnetic analysis data show the presence of a hard magnetic phase with $T_c = 250 \pm 5$ °C and $H_c = 4.8$–5.2 kOe for an as-cast $Nd_{80}Fe_{15}B_5$ sample. This is consistent with the results of Schneider *et al.*[9] Upon cooling from 600 °C, a new phase develops with a $T_c = 318 \pm 5$ °C and $H_c = 10$–16 kOe. The sample with $x = 25$ had the latter phase in the as-cast state. In the sample with $x = 20$, the high T_c phase developed during the heating cycle to 600 °C [double peak in Fig. 1(a)]. Table I lists corresponding coercivities and saturation mag-

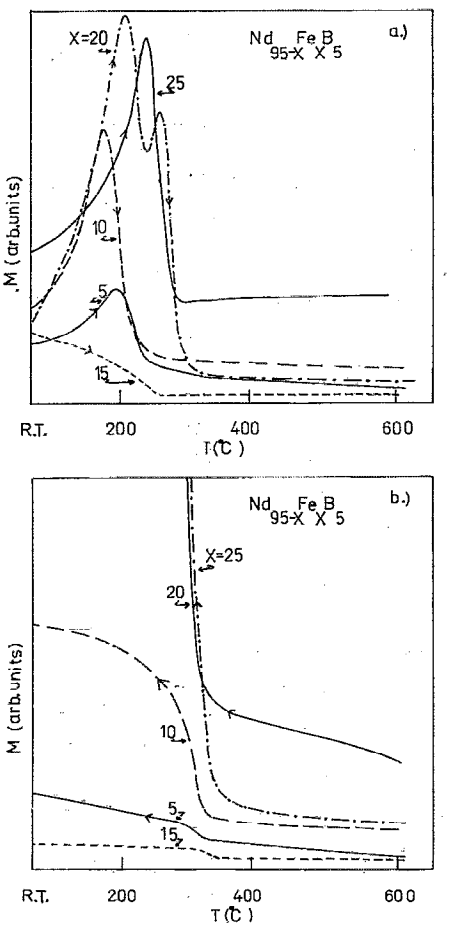

FIG. 1. Thermomagnetic curves for $Nd_{95-x}Fe_xB_5$ in a static field of 800 Oe. (a) Heating cycle; (b) cooling cycle.

 0021-8979/91/085820-03$03.00

TABLE I. Magnetic properties for $Nd_{95-x}Fe_xB_5$ alloys.

Sample	As-cast		After heat treatment at 600 °C	
	M_s[a] (emu/g)	H_c (kOe)	M_s[a] (emu/g)	H_c (kOe)
$Nd_{90}Fe_5B_5$	2.61	4.0	4.63	3.6
$Nd_{85}Fe_{10}B_5$	5.92	4.8	6.34	10.5
$Nd_{80}Fe_{15}B_5$	8.93	4.8	11.78	11.2
$Nd_{75}Fe_{20}B_5$	12.00	4.6	20.79	9.9
$Nd_{70}Fe_{25}B_5$	15.10	1.8	28.86	3.25

[a]Value of magnetization at 14 kOe.

netization, determined from VSM data. Coercivities are larger when measured with the SQUID magnetometer due to the higher saturating fields available (55 kOe).

Various heat treatments show that the coercivity in these alloys is critically dependent on the annealing temperature and cooling rates. The cooling rate probably determines the structure morphology of the sample especially the size and distribution of the hard magnetic phase.

Samples were homogenized at various temperatures around 700 °C where the DTA data show a phase transition and were quenched in water or cooled to room temperature at 1.5 °C/min. These samples underwent further annealing at 600 °C and were quenched in water or cooled to room temperature at 2.5 °C/min. The samples which were slow cooled from 850 °C show low coercivities. The quenched samples have nearly the same H_c as the as-cast samples with the exception of $Nd_{70}Fe_{25}B_5$ whose coercivity increases from 1.8 to 4.8 kOe after homogenizing and quenching. Optimal coercivities found using these heat treatments were much lower than in samples simply heated to near 600 °C during the thermomagnetic analysis experiment.

The best results were found in $Nd_{80}Fe_{15}B_5$ and this sample was chosen for further characterization. The magnetization curves for an as-cast and heat-treated sample are shown in Fig. 2. The initial magnetization curve of as-cast samples is more characteristic of noninteracting and randomly distributed single-domain particles. The initial curve of heat-treated samples resembles those of melt-spun Nd-Fe-B magnets and is characteristic of interacting single domain particles. The hysteresis loops for both of these samples are shown in Fig. 3. The coercivity and high field susceptibility are much higher in the heat-treated samples indicating a much higher anisotropy for the heat-treated samples consistent with the $Nd_2Fe_{14}B$ phase. Low-temperature thermomagnetic data (Fig. 4) show an increase in magnetization at around 140 and 50 K. The first temperature corresponds to the spin reorientation temperature of $Nd_2Fe_{14}B$,[11] whereas the lower temperature might be related with the ordering temperature of $FeNd_2B_3$.[9] These results are consistent with the $H_c(T)$ data which show the expected decrease in coercivity below 140 K (Fig. 4) because of the spin reorientation.

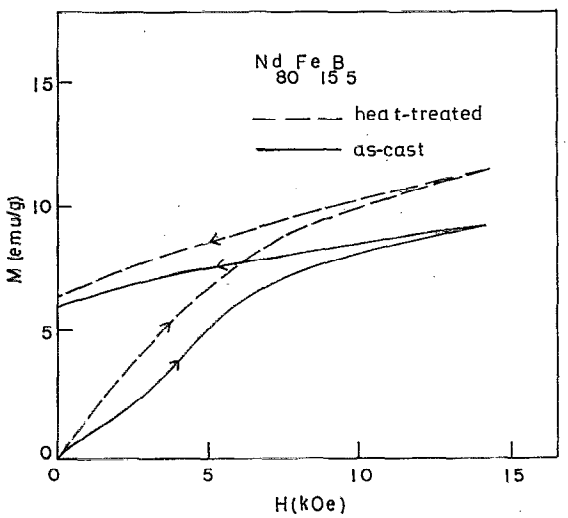

FIG. 2. Initial curve for $Nd_{80}Fe_{15}B_5$ for as-cast and heat-treated samples.

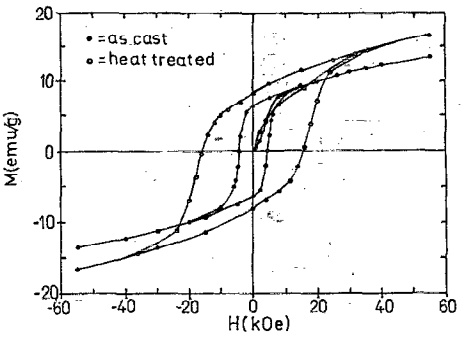

FIG. 3. Hysteresis curve for $Nd_{80}Fe_{15}B_5$ for as-cast and heat-treated samples.

X-ray analysis and selected area diffraction of as-cast and heat-treated samples show patterns characteristic of multiphase samples. At this time, the phases present have not been positively identified. The majority phase matches the Nd_2O_3 hexagonal phase.

Microstructure studies by SEM reveals a dendrite network in both as-cast and annealed samples. After annealing, the continuous dendrites dissolve into particles as shown in Fig. 5(a). The length of the dendrite is in the range of 10–20 μm, while the size of the particles formed from the dendrites is about 2–5 μm. Energy dispersive spectroscopy (EDS) results show that the particles are

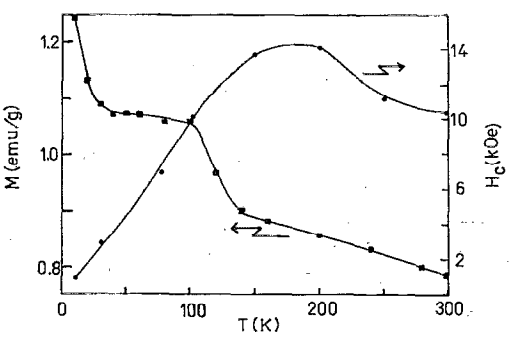

FIG. 4. Coercivity and thermomagnetic curves in the $Nd_{80}Fe_{15}B_5$ for a temperature range of 10–300 K.

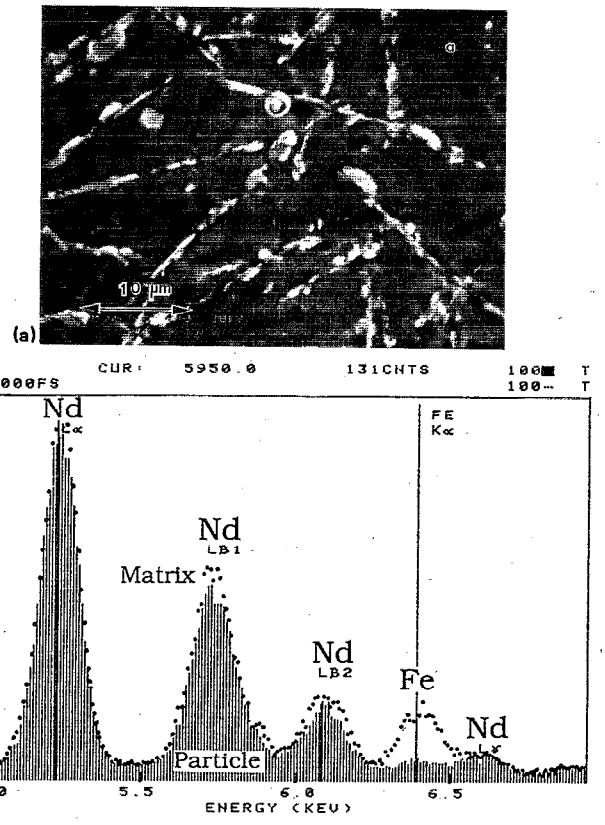

FIG. 5. (a) SEM micrograph revealing needle-like particles in a heat-treated $Nd_{80}Fe_{15}B_3$ sample. (b) EDS results for the same sample.

richer in Nd as compared to the area of matrix adjacent to it. The chemical composition of these regions is shown in Fig. 5(b).

TEM results reveal futher sets of fine needle particles in the grains of annealed samples, as shown in Fig. 6. The needles observed inside the grains have a preferential orientation with respect to the grain and appear or disappear as a whole when the grain is properly tilted. The size of these fine needles is about 100 Å and are believed to be the 2:14:1 phase which is responsible for the high coercivity.

IV. DISCUSSION

The x-ray diffraction patterns are complex consisting of several phases and due to the low volume fraction of the precipitates found in the annealed samples the structure of the hard magnetic phase is difficult to be identified. The magnetic results $[M_H(T), H_c(T)]$, however, support the hypothesis of the $Nd_2Fe_{14}B_1$ phase in *annealed* Nd-Fe-B samples. The hard magnetic phase in the *as-cast* Nd-Fe-B samples is assumed to be the metastable phase reported in as-cast Nd-Fe samples. Both of these phases are in the form of small precipitates which are randomly distributed in a nonmagnetic matrix. For a random distribution of single domain particles with uniaxial anisotropy the coercivity is given by

$$H_c = 0.96K/M_s, \tag{1}$$

where K is the anisotropy constant and M_s the saturation magnetization. Using the values of M_s, K ($H_A = 2K/M_s$) reported for the metastable phase ($M_s = 750$ emu/cc, $H_A = 19$ kOe) and the 2:14:1 phase ($M_s = 1270$ emu/cc, $H_A = 68$ kOe), the predicted coercivities according to Eq. (1) are 9.0 and 32.6 kOe, respectively. These values are larger than the experimentally observed maximum values (5.2 and 16 kOe, respectively). This may be due to several reasons including particle interactions, incoherent processes,[12] and domain-wall pinning in the large particles.

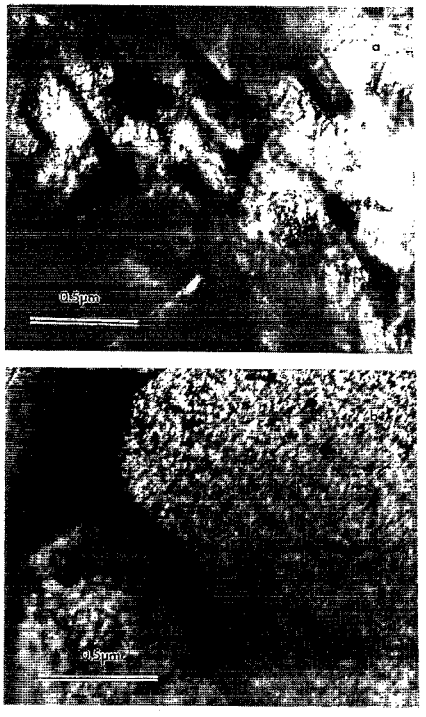

FIG. 6. Needle-shaped particles within sample grains and grain boundaries of heat-treated $Nd_{80}Fe_{15}B_5$.

ACKNOWLEDGMENTS

This work has been supported by the National Science Foundation under Grant No. DMR-8917028.

[1] A. Tsoukatos, J. Strzeszewski, and G. C. Hadjipanayis, J. Appl. Phys. **64**, 5971 (1988).
[2] G. Schneider, G. Martinek, H. H. Stadelmaier, and G. Petzow, Mater. Lett. **7**, 215 (1988).
[3] G. C. Hadjipanayis, A. Tsoukatos, J. Strzeszewski, G. J. Long, and O. A. Pringle, J. Magn. Magn. Mater. **78**, L1 (1989).
[4] F. A. O Cabral, R. S. Turtelli, S. Gama, and F. L. A. Macahado, IEEE Trans. Magn. **25**, 3318 (1989).
[5] J. L. Sanchez Llamazares, F. Leccabue, F. Leccabue, F. Bolzoni, R. Panizzieri, and Xue Ron Hua, J. Magn. Magn. Mater. **84**, 79 (1990).
[6] J. L. Sanchez Llamazares, F. Calderon, F. Bolzoni, F. Leccabue, Xue Rong Hua, and J. P. Nozieres, J. Magn. Magn. Mater. **86**, 307 (1990).
[7] G. Schneider, F. J. G. Landgraf, V. Villas-Boas, G. M. Bezerra, F. P. Missell, and A. E. Ray, Mater. Lett. **8**, 472 (1989).
[8] G. Schneider, F. J. G. Landgraf, V. Villas-Boas, and F. P. Missell, *Proceedings of the 10th International Workshop on Rare-Earth Magnets and Their Applications* (Society for Non-Traditional Techniques, Tokyo, 1989), Vol. 1, pp. 63–72.
[9] G. Schneider, F. J. G. Landgraf, and F. P. Missell, J. Less Common Metals **153**, 169 (1989).
[10] J. M. Moreau, L. Paccard, J. P. Nozieres, F. P. Missell, G. Schneider, and V. Villas-Boas, J. Less Common Metals (to be published).
[11] D. Givord, H. S. Li, and J. M. Moreau, Solid State Commun. **50**, 497 (1984).
[12] H. Zijlstra, in *Ferromagnetic Materials*, edited by E. P. Wohlfarth (North-Holland, Amsterdam, 1982), Vol. 3, pp. 37–105.